ACS Synthetic Biology

Letter

Cite This: ACS Synth. Biol. 2019, 8, 937−947

pubs.acs.org/synthbio

One-Pot Assembly of Complex Giant Unilamellar Vesicle-Based Synthetic Cells

Kerstin Göpfrich,[†,‡] Barbara Haller,[†,‡] Oskar Staufer,[†,‡] Yannik Dreher,[†,‡] Ulrike Mersdorf,[¶] Ilia Platzman,[*,†,‡] and Joachim P. Spatz[*,†,‡]

[†]Max Planck Institute for Medical Research, Department of Cellular Biophysics, Jahnstraße 29, D 69120, Heidelberg, Germany

[‡]Department of Biophysical Chemistry, University of Heidelberg, Im Neuenheimer Feld 253, D 69120 Heidelberg, Germany

[¶]Max Planck Institute for Medical Research, Department of Biomolecular Mechanisms, Jahnstraße 29, D 69120, Heidelberg, Germany

Supporting Information

ABSTRACT: Here, we introduce a one-pot method for the bottom-up assembly of complex single- and multicompartment synthetic cells. Cellular components are enclosed within giant unilamellar vesicles (GUVs), produced at the milliliter scale directly from small unilamellar vesicles (SUVs) or proteoliposomes with only basic laboratory equipment within minutes. Toward this end, we layer an aqueous solution, containing SUVs and all biocomponents, on top of an oil−surfactant mix. Manual shaking induces the spontaneous formation of surfactant-stabilized water-in-oil droplets with a spherical supported lipid bilayer at their periphery. Finally, to release GUV-based synthetic cells from the oil and the surfactant shell into the physiological environment, we add an aqueous buffer and a droplet-destabilizing agent. We prove that the obtained GUVs are unilamellar by reconstituting the pore-forming membrane protein α-hemolysin and assess the membrane quality with cryotransmission electron microscopy (cryoTEM), fluorescence recovery after photobleaching (FRAP), and zeta-potential measurements as well as confocal fluorescence imaging. We further demonstrate that our GUV formation method overcomes key challenges of standard techniques, offering high volumes, a flexible choice of lipid compositions and buffer conditions, straightforward coreconstitution of proteins, and a high encapsulation efficiency of biomolecules and even large cargo including cells. We thereby provide a simple, robust, and broadly applicable strategy to mass-produce complex multicomponent GUVs for high-throughput testing in synthetic biology and biomedicine, which can directly be implemented in laboratories around the world.

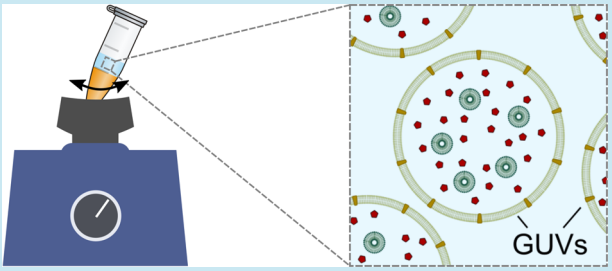

KEYWORDS: *giant unilamellar vesicles (GUVs), water-in-oil droplets, synthetic cells, bottom-up assembly, protocells, proteoliposomes*

Lipid bilayer membranes define the boundaries of virtually all living cells. The creation of artificial phospholipid vesicles gave insights into the biophysical properties of cellular membranes and led to the development of new drug delivery systems.[1] Giant unilamellar vesicles (GUVs), in particular, have become increasingly popular model systems in bottom-up synthetic biology, since they match the dimensions of eukaryotic cells and can conveniently be monitored with light microscopy on the single-compartment level. They serve as biomimetic compartments for the encapsulation and reconstitution of cellular components *in vitro*, shedding light on their function in a well-defined environment isolated from the complexity of a living cell.[2−4] While several key milestones toward the assembly of a synthetic cell have been accomplished,[5] there is a key problem to be addressed for the full flourishing of the field: Increasingly complex cell-like systems require methods for efficient encapsulation of multiple components inside compartments at high yield. Despite the widespread use of GUVs, for synthetic biology as well as biomedical applications, there are still challenges regarding their formation.

Initially, the gentle hydration approach was proposed for GUV formation.[6] A dried lipid film was exposed to an aqueous solution for hours and days at temperatures above the phase transition temperature of the lipids.[7] A major improvement to this protocol was suggested by Angelova and Dimitrov: By applying an external electric ac-field to the lipid solution, larger GUVs could be obtained (above 30 μm diameter) and the formation process was sped up.[8] This so-called electroformation approach is still the most commonly used method for GUV formation. It is well characterized and was developed further to increase its versatility, e.g., to improve compatibility with charged lipids.[9] Nevertheless, the yield is optimal for uncharged lipids and nonphysiological salt concentrations, as charges usually interfere with the process. Natural cell

Received: January 28, 2019
Published: May 1, 2019

DOI: 10.1021/acssynbio.9b00034
ACS Synth. Biol. 2019, 8, 937−947

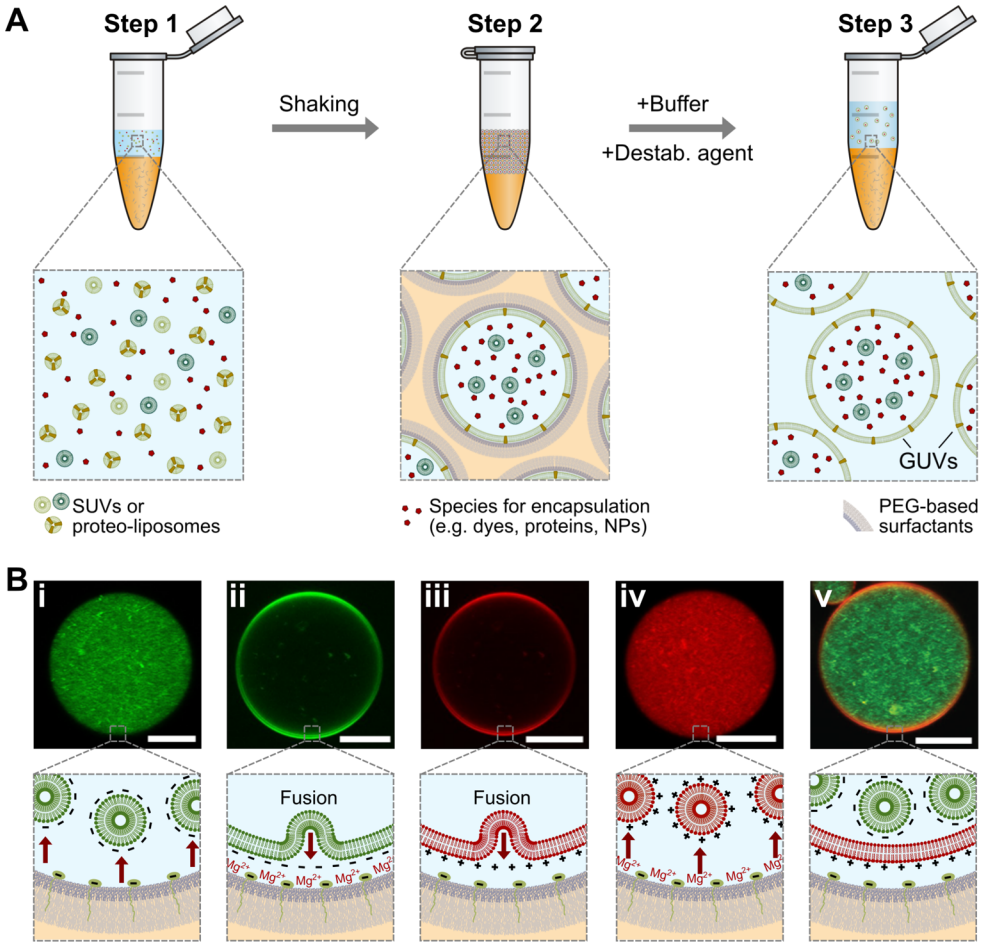

Figure 1. (A) Schematic illustration of the 3-step "shaking" strategy for the formation of GUV-based synthetic cells. Step 1: An aqueous solution containing the SUVs and/or proteo-liposomes and the species for entrapment is layered on top of fluorinated oil supplemented with PEG-based fluorosurfactants. Step 2: Manual shaking or vortexing induces the formation of surfactant-stabilized water-in-oil droplets. SUVs and proteo-liposomes fuse to form a spherical supported lipid bilayer at the droplet interface (termed droplet-stabilized GUVs, dsGUVs). Step 3: Upon addition of an aqueous buffer and a droplet destabilizing agent, GUVs are released from the surfactant shell and the oil phase into the aqueous buffer. (B) Confocal fluorescence images and schematics illustrating the conditions for the charge-mediated formation of dsGUVs. In the absence of Mg^{2+}, negatively charged SUVs (here, 30% DOPG, green) remain homogeneously distributed inside the droplet (i), while dsGUVs are formed in the presence of Mg^{2+} (10 mM, ii). The opposite is true for positively charged SUVs (here, 30% DOTAP, red, iii and iv). Multicompartment GUVs can be formed from a mixture of positively (red) and negatively (green) charged SUVs (v). Note that SUVs are smaller than the diffraction limit and that the droplet interface is negatively charged due to the presence of Krytox (10.5 mM, light green in illustration). Scale bars: 10 μm.

membranes, however, typically include a significant amount of negatively charged lipids (around 30%).[10] Additionally, the encapsulation efficiency of biomolecules is low, making it difficult to assemble complex synthetic cells. Alternatives have been proposed, including solvent evaporation,[11] osmotic shock,[1] gel-assisted swelling,[7] and inverted emulsions.[12] A good overview of these techniques and potential artifacts can be found elsewhere.[13,14] Notably, the water-in-oil emulsion transfer method[15] greatly improved the encapsulation efficiency, which led to the successful reconstitution of protein expression systems in GUVs.[16] Recently, different methods for the microfluidic formation of GUVs were demonstrated.[17−22] These methods received increased attention for the bottom-up assembly of synthetic cells, as they feature high-yield and homogeneous size, and most importantly, encapsulation of biomolecules *via* the aqueous inlet is straightforward.[23] However, establishing microfluidic technologies may be time-consuming and, in the case of PDMS-based microfluidics, requires clean room facilities. While glass-capillary microfluidics[20] circumvents the need for a clean room, this method uses a relatively expensive capillary preparation technology. Alignment of the capillaries and their sealing is a laborious process. Moreover, in both cases, when there are interactions between the microfluidic channel walls and the species for encapsulation, forming stable GUVs can be challenging.

Here, we propose a simple and cost-effective one-pot method to produce GUV-based single- and multicompartment systems for synthetic biology and biomedical applications. Like the microfluidic method proposed by Weiss *et al.*,[21] it relies on the charge-mediated fusion of SUVs or proteoliposomes inside surfactant-stabilized droplets[22] yet circumvents the need for microfluidic technologies. The developed method requires only the most basic equipment and produces GUVs on the milliliter scale within minutes, making it suitable for high-throughput testing and well-plate formats. It is compatible with a broad range of buffer conditions, such as buffers with high ionic strength and cell medium, and offers a flexible choice of lipid compositions, including high molar fractions of charged lipids. Most notably, the GUV formation method features a

DOI: 10.1021/acssynbio.9b00034
ACS Synth. Biol. 2019, 8, 937−947

straightforward reconstitution of membrane proteins and formation of multicompartment systems as well as high encapsulation efficiency.

RESULTS AND DISCUSSION

Shaking Strategy for the Formation of GUV-Based Synthetic Cells. Figure 1 illustrates the one-pot formation of multicomponent GUV-based synthetic cells step by step. To this end, we prepare an aqueous buffer solution containing SUVs and/or proteoliposomes as well as all compounds for encapsulation in the GUVs. We layer this aqueous solution on top of a mixture of fluorinated oil and a PEG-based fluorosurfactant (Step 1, Figure 1A). Vigorous vortexing or manual shaking induces the formation of surfactant-stabilized water-in-oil droplets, encapsulating the SUVs and the other components in the aqueous phase. Under appropriate conditions as described in the next paragraph, it is possible to trigger the charge-mediated fusion of the SUVs at the droplet periphery leading to the formation of a spherical supported lipid bilayer (Step 2, Figure 1A). We hence obtain a GUV inside the water-in-oil droplet, which we will refer to as "droplet-stabilized GUV" (dsGUV, consistent with the terminology used in earlier work where dsGUVs were obtained by means of microfluidics[21,22]). If the outer aqueous phase is not required, dsGUVs may already be sufficient for further experimentation. To form freestanding GUVs and to release the GUVs from the droplet's surfactant shell and the oil phase, we add the desired aqueous buffer and a droplet-destabilizing agent (Step 3, Figure 1A). As a droplet-destabilizing agent, we use perfluoro-1-octanol (PFO), a surfactant with a shorter chain-length that is displacing the stabilizing surfactants at the droplet periphery. This leads to the fusion of the droplets at the interface between the oil and the aqueous buffer. Once the surfactant shell is opened up, the intact GUVs are released into the aqueous buffer. Note that successful release is only possible if the droplets encapsulate an appropriate amount of SUVs, providing full coverage of the droplet interface with a lipid bilayer. We calculated the required lipid concentration for different droplet sizes and plotted it in the Supporting Information (Figure S1, Text S2). Detailed step-by-step instructions with tips for troubleshooting and a video protocol of the entire GUV formation process are also provided in the Supporting Information (Text S1, Video S1).

Functional modules for synthetic cells have different prerequisites in terms of lipid compositions and buffer conditions. To ensure compatibility of our method with a diverse range of applications, we set out to form GUVs from SUVs composed of different types of charged and uncharged lipids under diverse buffer conditions. It is important to consider that with out method, the GUV formation process initially requires the formation of a supported lipid bilayer (SLB) at the droplet periphery (Figure 1B). SLB formation on solid state supports has been studied in detail. It is driven by van der Waals and electrostatic interactions between the SUVs and the support,[24−26] in our case the surfactant layer. Therefore, for successful GUV formation, one needs to consider the interplay of the charges present in the system: 1, charged lipids; 2, ions in the buffer; and 3, charged surfactants presented at the droplet interface. In the absence of charged surfactants at the droplet interface, e.g., if the droplets are stabilized by inert PEG-based fluorosurfactants, no fusion of the SUVs is observed (see the Supporting Information, Figure S2). Also when using a sufficient amount of negatively charged surfactants, e.g., Krytox,[22] negatively charged SUVs remain homogeneously distributed inside the droplet as visible in the confocal image and the illustration in Figure 1B,i. Note that the measured diameter of the SUVs lies around 60 nm (determined by dynamic light scattering measurements, see the Supporting Information, Figure S3) and thus below the optical diffraction limit. Therefore, individual SUVs cannot be resolved by conventional optical microscopy. Formation of negatively charged dsGUV is successful in the presence of Mg^2+ ions since the Mg^{2+} ions are capable of screening the negative charges, as visually indicated by the bright ring in the confocal plane, see Figure 1B,ii. Alternatively, an increased concentration of monovalent ions (100 mM) can be used to achieve dsGUV formation.[22] The formation of dsGUVs from positively charged SUVs, on the other hand, is only possible in the absence of Mg^{2+} ions (Figure 1B,iii,iv). Most remarkably and importantly, this provides a direct route for the formation of multicompartment systems (vesosomes) with distinct lipid compositions as demonstrated in Figure 1B,v: If a mixture of positively and negatively charged SUVs is encapsulated during the shaking process in the absence of Mg^{2+}, the positively charged SUVs fuse at the droplet periphery to form the large outer GUV compartment. The negatively charged SUVs, on the other hand, are not attracted to the droplet periphery under these conditions and hence small internal compartments remain. Note that we do not observe fusion of the oppositely charged SUVs as has been reported before.[27] This may be due to the lack of ions in the buffer. We thus demonstrate that the shaking method for GUV formation can separate SUVs according to their charge. While SUVs have previously been encapsulated in GUVs,[22] to our best knowledge we demonstrate the first multicompartment system where internal and external compartments are made of different lipids. Multicompartment systems with segregated volumes can decouple reactions inside complex synthetic cells or drug carriers. They are also relevant as mimics of eukaryotic cell architecture, featuring membrane-bound organelles enclosed by a larger compartment.

Characterization of GUVs Formed by the Shaking Strategy. To validate the proposed strategy for synthetic cell assembly, we first used the shaking method to form plain free-standing GUVs in an aqueous buffer without membrane proteins or encapsulated species. Figure 2A shows dsGUVs produced by vortexing of an oil and an aqueous phase for 10 s. The aqueous phase contained SUVs composed of 30% negatively charged lipids (1.2 mM lipids, 30% DOPG, 34.75% DOPC, 34.75% POPC, supplemented with 0.5% Atto488-labeled DOPE for visualization purposes) in a 10 mM $MgCl_2$-containing Tris buffer (30 mM Tris, pH 7.4). To trigger the charge-mediated fusion of the SUVs and the formation of dsGUVs, the oil phase (containing 1.4 wt % of a commercially available PEG-based fluorosurfactant in HFE-7500) was supplemented with a negatively charged perfluoropolyether (PFPE) carboxylic acid fluorosurfactant (10.5 mM Krytox).[22] Under these conditions, the dsGUV formation was successful, visually indicated by the bright ring in the confocal plane (Figure 2A). Note that without the negatively charged surfactant or without $MgCl_2$, the SUVs remain homogeneously distributed within the droplet (see Figure 1B,i and the Supporting Information, Figure S2) and the release of GUVs is not possible. Figure 2B shows the GUVs after their successful release from the oil phase and the surfactant shell into an aqueous buffer (10 mM $MgCl_2$, 30 mM Tris, pH 7.4).

DOI: 10.1021/acssynbio.9b00034
ACS Synth. Biol. 2019, 8, 937−947

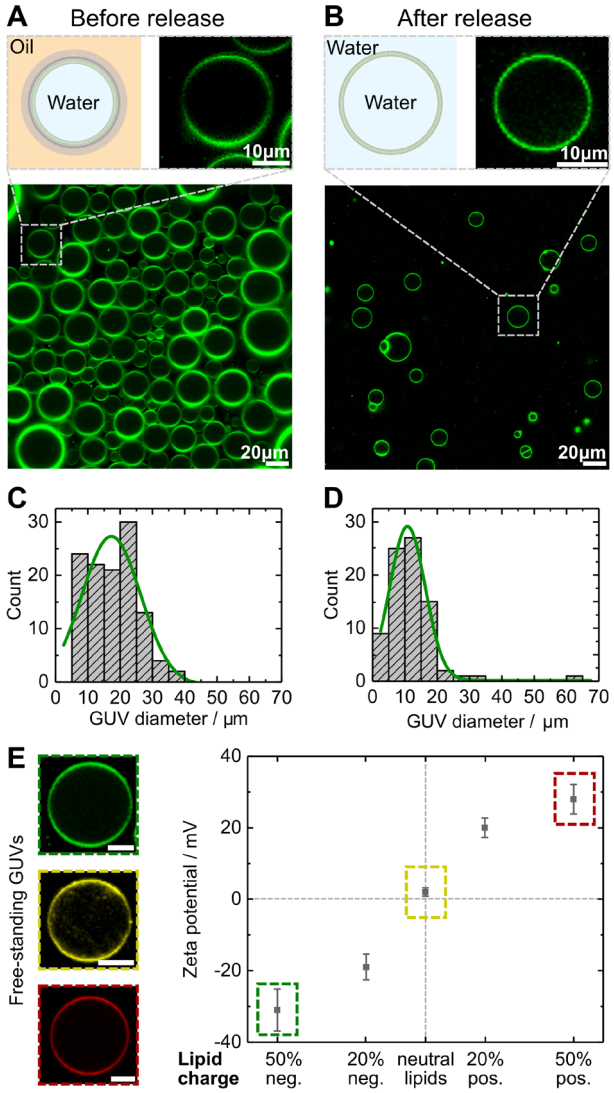

Figure 2. Formation of free-standing GUVs *via* the shaking method. (A) Confocal fluorescence imaging of droplet-stabilized GUVs obtained after encapsulation of SUVs into water-in-oil droplets *via* the shaking method. Oil phase: 1.4 wt % PEG-based fluorosurfactant, 10.5 mM Krytox in HFE. Aqueous phase: 1.2 mM lipidmix (SUVs made of 30% DOPG, 15% cholesterol, 27.25% DOPC, 27.25% POPC, 0.5% Atto488-labeled DOPE) in 10 mM $MgCl_2$, 30 mM Tris, pH 7.4. (B) Free-standing GUVs after release. (C) Histogram showing the size distribution of the droplet-stabilized GUVs produced by the shaking method before release. (D) Histogram of the size distribution of free-standing GUVs after release. The size distribution was analyzed with ImageJ using manual thresholding and the particle analysis tool. (E) Confocal fluorescence imaging (left, scale bars, 10 μm) and zeta potential measurements (right) of free-standing GUVs produced from SUVs with different mol % of charged lipids: up to 50% negatively charged lipids (green, DOPG in 10 mM $MgCl_2$, 30 mM Tris), neutral lipids (yellow, 50% DOPC, 50% POPC in 100 mM KCl, 30 mM Tris), and up to 50% positively charged lipids (red, DOTAP in 30 mM Tris). 0.5 mol % Atto488-labeled DOPE or LissRhod-PE was added to the lipid mixture for visualization purposes.

As expected, GUVs in close proximity adhere to one another because of their negative charge and the presence of magnesium ions in the buffer.[28] This can be circumvented by replacing $MgCl_2$ with an osmolarity-matched sugar solution (e.g., 30 mM glucose instead of 10 mM $MgCl_2$).

The histograms in Figure 2C,D show the size distribution of the GUVs before (C) and after release (D) under the described conditions. The mean diameter of the GUVs after release lies at around 10 μm. The more narrow size distribution after the release can be explained by the fact that the more unstable large GUVs tend to burst during the release process or to fuse with the coverslide. While the GUV dimensions are not monodisperse and fully controllable as with microfluidic methods, there are several factors that determine their size: Manual shaking produces larger GUVs than vortexing which, in turn, produces larger GUVs than emulsification. Additionally, surface tension affects the GUV diameter, which depends on the specific combination of surfactant, buffer conditions, and encapsulated species. Note that while the release of GUVs is possible immediately after dsGUV formation, higher yield can be achieved if the dsGUVs are left to equilibrate overnight at 4 °C. Especially when only monovalent ions are used, it can take several hours until the SUVs completely fuse at the droplet periphery forming a homogeneous lipid bilayer. Depending on the buffer conditions, overnight equilibration therefore increases the amount of GUVs by approximately 50−200%.

By counting the GUVs in the confocal plane as described in the Supporting Information (Figure S4, Text S3), we estimate the yield of the GUV production. With just 1 mL of the aqueous phase, our method can produce over 10^7 GUVs. Approximately 10% of the droplets were released successfully after overnight incubation. Since the shaking method can easily be scaled up to the milliliter scale and beyond, a relatively low release rate does not set a particular limit to the overall amount of obtained GUVs. The scalability of the shaking method is of special interest for biomedical applications of GUVs, in particular drug delivery. While liposomal drug delivery currently employs small liposomes rather than GUVs (<200 nm in diameter[1]), larger compartments will become necessary for loading more sophisticated large cargos. These include nano/microparticles or supramolecular DNA complexes that offer great potential for future therapeutic approaches.[29] We envision that GUV-based drug carriers could be administered subcutaneously or transdermaly, e.g., for wound healing, used as synthetic cell implants or potentially be injected intravenously, if they can deform sufficiently in narrow capillaries.

To test if highly charged GUVs can also be successfully released from the oil phase into an aqueous environment, we performed confocal fluorescence imaging experiments and zeta potential measurements. Figure 2E (left) shows free-standing GUVs made of highly negatively charged lipids (50 mol % DOPG, green), neutral lipids (DOPC/POPC, yellow), and highly positively charged lipids (50 mol % DOTAB, red). GUVs composed of similarly high fractions of charged lipids are difficult to obtain with electroformation.[9] In the case of neutral lipids, their polar headgroup is sufficient to trigger the charge-mediated fusion at the droplet interface. To probe whether certain types of lipids may be leaking into the oil phase rather than being incorporated into the GUV, we performed zeta-potential measurements for GUVs formed from SUVs containing different percentages of charged lipids. As plotted in Figure 2E (right), the measured charge of the released GUVs corresponds to the charge of the SUVs. A comparison of the zeta-potentials of SUVs and GUVs is plotted in the Supporting Information (Figure S8). We thereby confirmed that the shaking method for GUV formation is suitable to form neutral as well as highly charged GUVs.

DOI: 10.1021/acssynbio.9b00034
ACS Synth. Biol. 2019, 8, 937−947

Furthermore, we successfully tested diverse lipid compositions including lipids like DOPC, POPC, DOPG, DOTAB, EggPC, EggPG, EggPA, cholesterol, and even *E. coli* polar lipid extract (for a tabular overview and confocal images see the Supporting Information, Table S1 and Figure S6). The shaking method for GUV formation is compatible with a diverse range of different buffers, including sucrose/glucose, pure water, sorbitol, magnesium chloride, sodium chloride, PBS, or even full medium (DMEM with 10% FBS) (see tabular overview and confocal images in the Supporting Information, Table S1 and Figure S6). All conditions listed in Table S1 were optimized to give release rates of at least 2%. Best release rates were obtained for EggPC/EggPG lipids and in the absence of magnesium ions in the release buffer (up to 50%, see Figure S6). Considering that the shaking method can produce GUVs on the milliliter scale, a low release rate still provides a remarkable amount of GUVs. When testing new conditions that are not described here, to achieve the best possible results, we advise to consult the extensive literature on the formation of SLBs[24−26] and to screen the parameter space for an optimal combination of lipids, buffer, and Krytox concentration.

Confirmation of Unilamellarity. Unilamellarity of the compartment membrane is a prerequisite for the functional incorporation of transmembrane proteins, an important aspect to establish signaling between synthetic cells and the surrounding environment. We therefore set out to assess the membrane quality and the unilamellarity of the GUVs produced *via* shaking. First, we performed fluorescence recovery after photobleaching (FRAP) measurements to determine the fluidity of the membrane. A circular bleaching area was selected at the top of the vesicle (opposite to the area where the vesicle is in contact with the cover slide) and the fluorescence intensity within this confocal plane was recorded over time. Figure 3A shows confocal fluorescence images (inset) and a plot of the fluorescence intensity before and directly after bleaching, as well as after recovery (12 s time point). We obtained a diffusion coefficient of 2.30 ± 0.25 $\mu m^2/s$, determined from an exponential fit of the intensities during the recovery period. This value is in very good agreement with literature values for GUVs with a similar membrane composition.[30]

CryoTEM measurements were performed to visualize the membrane lamellarity of the released vesicles. Figure 3B shows a cryoTEM micrograph of a vesicle that we produced *via* the shaking method. The zoom image unambiguously confirms its unilamellarity.

Moreover, to provide an independent proof of unilamellarity, we added the protein nanopore α-hemolysin[31] externally to the preformed GUVs and carried out dye influx experiments using fluorescein as a fluorescence probe. Since the protein pore can only span a single lipid bilayer, no dye influx would be observed for multilamellar vesicles. In a unilamellar vesicle, on the other hand, the nanopore will create a passage for the polar dye, which can then permeate into the vesicle along its concentration gradient. In the presence of the nanopores, the fluorescence intensity inside the GUVs increased within a few minutes as visible in the representative confocal image and the plot in Figure 3C, confirming the unilamellarity of the lipid membrane. In the absence of the nanopores, the GUVs remained dark (Figure 3D) as expected since fluorescein is polar and hence mostly membrane impermeable under the conditions we used. It should be noted that the experiments

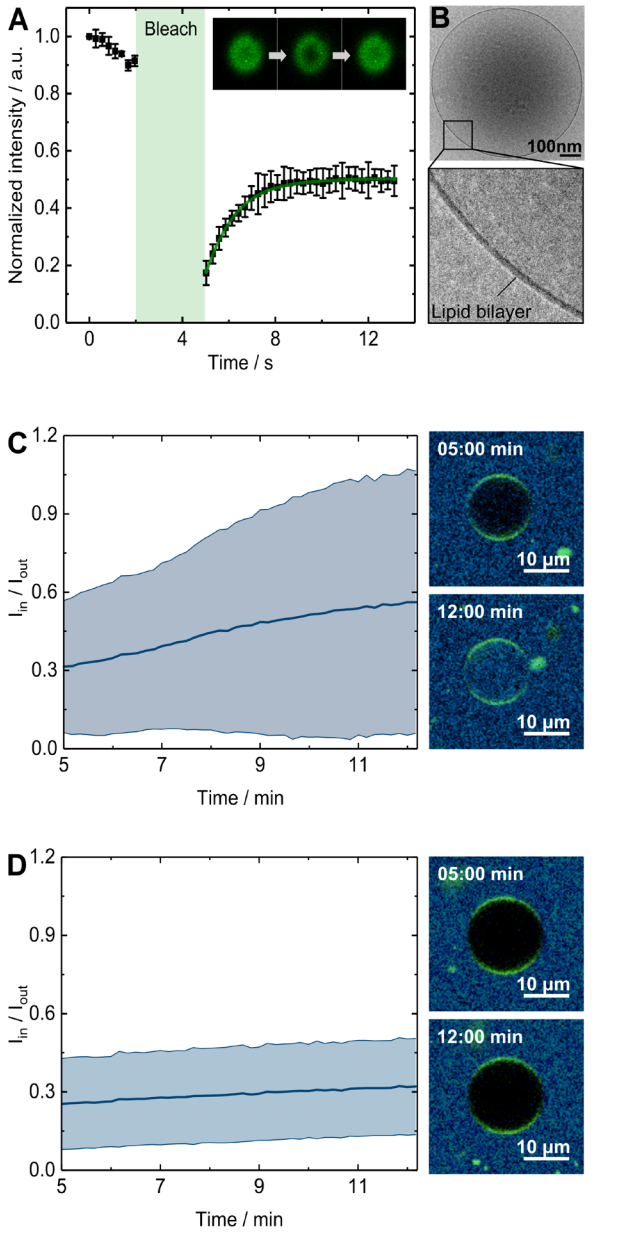

Figure 3. Confirmation of unilamellarity of GUVs produced *via* the shaking method. (A) FRAP measurements provide a diffusion coefficient of 2.30 ± 0.25 $\mu m^2/s$. Error bars correspond to the standard deviation of five independent measurements. (B) CryoTEM micrograph of a GUV (20% EggPG, 79% EggPC, 1% LissRhod-PE in PBS, 10 mM $MgCl_2$) showing the unilamellarity of the lipid bilayer. (C) Dye (fluorescein) influx measurements performed after addition of 10.7 nM heptameric α-hemolysin nanopores (75 nM monomers). Left: The mean intensity inside GUVs over the intensity outside of the GUVs (N = 25) is plotted as a function of time. The mean and the standard deviation are shown. Right: Representative confocal fluorescence images of a GUV at the beginning and the end of the measurement. (D) Dye influx measurements performed without addition of α-hemolysin nanopores. N = 28. Error bars correspond to the standard deviation.

were carried out at low α-hemolysin concentrations (10.7 nm heptameric pores) to avoid bursting of the GUVs. Under these conditions, inhomogeneities in the distribution of the α-hemolysin across the GUVs are expected and led to a wide spread of dye transport rates in the experiments. For a visual impression of the dye influx, see Video S2, and an individual

DOI: 10.1021/acssynbio.9b00034
ACS Synth. Biol. 2019, 8, 937−947

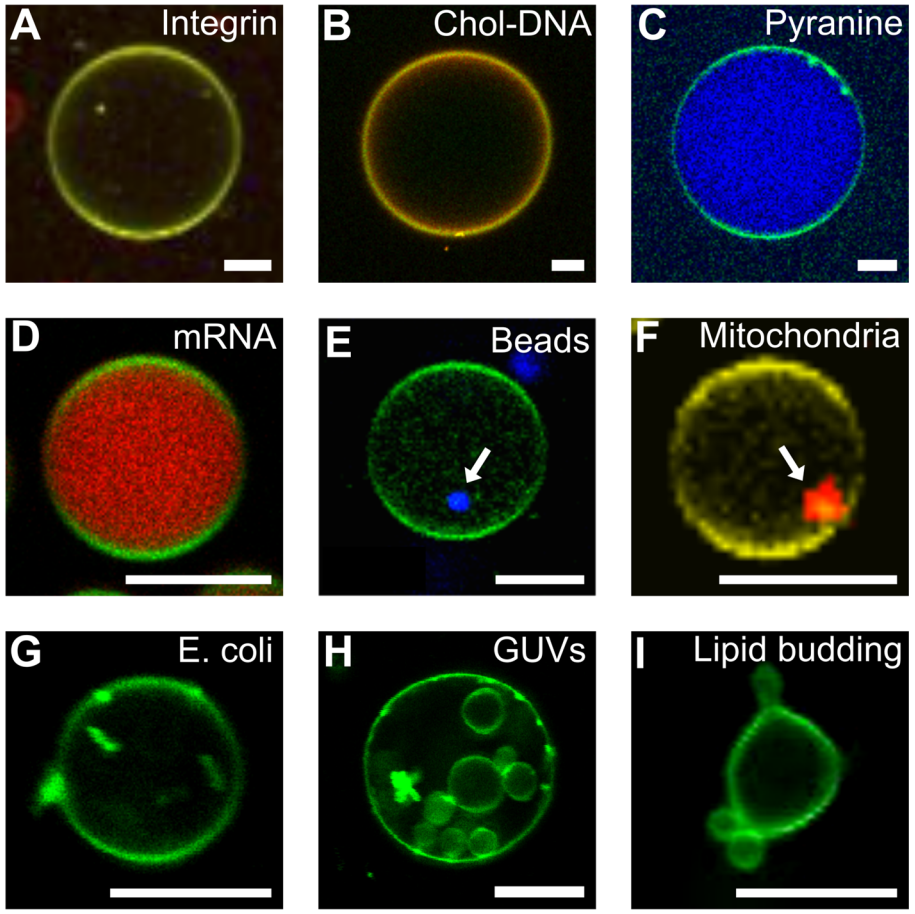

Figure 4. Confocal fluorescence images showing the diverse possibilities for encapsulation and reconstitution into the GUVs produced by the shaking method. Free-standing GUVs with (A) reconstituted TAMARA-labeled $\alpha_{IIb}\beta_3$ integrin; (B) Cy3-labeled membrane-adhering cholesterol-tagged DNA; (C) 100 nM encapsulated pyranine; (D) SYBR Green I-stained mRNA; (E) multifluorescent polystyrene beads; (F) mitochondria isolated from HeLa cells and stained with MitoTracker Green; (G) GFP-labeled *E. coli*; (H) GUVs; and (I) lipid budding and tube formation in osmotically deflated GUVs. Scale bars: 10 μm.

trace showing dye influx in the presence of the pores is plotted in the Supporting Information (Figure S7). When increasing the α-hemolysin concentration by 1 order of magnitude, the vast majority of the GUVs (≈95%, determined by confocal imaging and counting the GUVs before and after addition of α-hemolysin) burst within minutes.[32] The vesicles that remained intact (≈5%) are likely to be multilamellar. A similar fraction of multilamellar vesicles is obtained with the standard methods for GUV production.[33]

The results presented in this section indicate that the lipid membrane properties of GUVs produced *via* the shaking method do not differ noticeably from those formed by other means. Traces of oil, surfactant, and/or destabilizing agent were not detectable in the GUVs in bending rigidity measurements[21] and infrared (IR) and MALDI mass spectrometry (MS) measurements.[22] However, we cannot exclude the possibility that traces of the substances are present in the lipid membrane.

Reconstitution and Encapsulation. The most critical step toward the construction of synthetic cells, however, is the reconstitution of proteins and the encapsulation of diverse biocomponents inside the GUV. A particular advantage of our shaking method for GUV formation is the ease of membrane protein reconstitution by forming GUVs directly from SUVs. This is highly advantageous since the reconstitution of membrane proteins into SUVs is well established, while direct reconstitution in GUVs often remains problematic.[34] To illustrate this, we formed GUVs from proteo-SUVs containing the TAMRA-labeled transmembrane protein $\alpha_{IIb}\beta_3$ integrin as shown in Figure 4A. Note that the orientation of membrane protein insertion may be random, especially for proteins that lack large hydrophilic head groups. However, methods to control the directionality of the insertion are under active development and would be compatible with the shaking method for GUV formation.[35,36] Similarly, cholesterol-tagged DNA could be tethered to the membrane of the GUVs simply by forming the GUVs from DNA-functionalized SUVs (see Figure 4B). While GUVs have been functionalized with cholesterol-tagged DNA on the exterior, e.g., to trigger attachment of DNA nanopores[37−39] or membrane-bending DNA nanostructures,[40] this has never been achieved for the internal bilayer leaflet. Notably, cholesterol-tagged DNA handles at the GUV's interior could serve as addressable attachment handles to organize components inside synthetic cells.[41]

Another advantage of the shaking method is the high encapsulation efficiency of components inside the GUVs. Water-soluble components can simply be added to the aqueous SUV solution before shaking. We first demonstrated this by encapsulating a fluorescent dye (pyranine) inside the

DOI: 10.1021/acssynbio.9b00034
ACS Synth. Biol. 2019, 8, 937−947

GUVs (see Figure 4C), but likewise we achieved the encapsulation of biomacromolecules like mRNA (see Figure 4D). The size of the encapsulated species is not particularly limited: We achieved the encapsulation of fluorescent polystyrene beads, mitochondria isolated from living cells, and even *E. coli* inside the GUVs (see Figure 4E−G).

High encapsulation efficiency is not only desirable for synthetic cell assembly but also of great importance for biomedical applications of GUVs, in particular for drug delivery. Figure 4H,I shows the possibility to achieve complex membrane architectures including encapsulated GUVs and nonspherical lipid compartments obtained by osmotic deflation.[42] Such architectures are again relevant for more realistic cell mimics.

Note that all examples in Figure 4 are free-standing GUVs which have been released from the oil phase to mimic the physiological conditions. The shaking method, however, offers the additional opportunity to work with the dsGUV which are still surrounded by an oil phase and stabilized by surfactants. In this state, the compartment is highly stable and can easily be manipulated, e.g., *via* microfluidic pico-injection.[21] This will be advantageous for applications that do not require the external aqueous phase. Release into a physiological environment can still be performed at a later stage.

All these examples illustrate how versatile the shaking method for GUV formation is. This allows for the recombination of functional modules for synthetic cells, greatly enhancing the scope for complexity in the field.

CONCLUSION

We have presented a straightforward yet scalable shaking approach to form GUVs and highlighted its relevance for the assembly of increasingly complex synthetic cells as well as potential drug delivery systems. The shaking method for GUV formation is most closely related to the previously described droplet transfer method[15] and the microfluidic method for dsGUV formation.[21,22] Having characterized our GUVs and confirmed their unilamellarity *via* FRAP measurements, cryoTEM, and dye influx assays, we demonstrate the versatility of our shaking method by forming highly charged GUVs and GUVs with diverse lipid compositions under various buffer conditions. We then tested the compatibility of our method with versatile functional modules for synthetic cells. Notably, the reconstitution of the membrane protein is straightforward, since the shaking method allows for the formation of GUVs directly from SUVs, circumventing the more problematic direct reconstitution in GUVs.[34,43] While maintaining the same encapsulation efficiency as for microfluidic compartment formation, our method avoids complications related to the microfabrication of on-chip functions. We exemplify this point by encapsulating dyes, small and large vesicles, nucleic acids, microbeads, organelles, and even bacteria. The system offers maximum flexibility, as experiments can be performed in the droplet-stabilized state as well as on released GUVs, depending on whether compartment stability and manipulability is preferred or whether a physiological aqueous environment is necessary. The optimal method for GUV formation will always depend on the specific application. While the shaking method is broadly applicable, it does not come without limitations. As described, lipid composition, buffer conditions, and surfactant charge have to be matched such that the charge-mediated formation of a supported lipid bilayer is possible. This makes it challenging to form, e.g., negatively charged GUVs in the absence of cations, unless a positively charged surfactant is used. If components for encapsulation interact with the surfactant layer, the formation of a supported lipid bilayer may be inhibited. Although traces of oil or surfactant were not detectable in our GUVs, we cannot exclude their presence in the lipid membrane at low concentrations. Additionally, GUVs obtained *via* the shaking method are not monodisperse in size. If homogeneous size is required, filtering of the GUVs in the droplet-stabilized state is an option.[44,45] Note that dsGUVs can in principle be reinjected into a microfluidic device for further manipulation, e.g., *via* pico-injection, for observation or sorting.[2] This work, greatly scaling up and simplifying synthetic cell assembly, will lead to GUV-based multicomponent synthetic cells of unprecedented complexity, shifting paradigms for bottom-up synthetic biology. At the same time, the previously impossible high volume production of GUVs will pave the way for high-throughput screening assays, e.g., to test for drug transport in well plate formats and to develop novel smart drug delivery systems.

METHODS

SUV Formation. Atto488-labeled 1,2-dioleoyl-*sn*-glycero-3-phosphoethanolamine (Atto488-DOPE) was purchased from ATTO TEC (Germany) and cholesterol C8667 from Sigma-Aldrich (Germany). All other lipids were purchased from Avanti Polar Lipids, Inc. All aqueous buffers were purchased from Sigma-Aldrich (Germany). Lipids were stored in chloroform at −20 °C and used without further purification. SUVs with different lipid compositions were formed by mixing the lipids at the desired molar ratio in a glass vial and subsequently dried under a stream of nitrogen gas. To remove traces of solvent, the vial was kept under vacuum in a desiccator for at least 2 h. A solution of 30 mM Tris, pH 7.4 (if not mentioned otherwise) was added to resuspend the dried lipid film at a lipid concentration of 2.2 mM. The solution was vortexed for at least 10 min to trigger liposome formation and subsequently extruded to form homogeneous SUVs with seven passages through a polycarbonate filter with a pore size of 50 nm (Avanti Polar Lipids, Inc.). SUVs were stored at 4 °C for up to 3 days or used immediately for dsGUV formation.

GUV Formation. We initially prepared an aqueous solution containing SUVs (1.1 mM 30% DOPG, 34.75% DOPC, 34.75% POPC, 0.5% Atto488-DOPE) in 10 mM $MgCl_2$, 30 mM Tris, pH 7.4. The oil−surfactant mix contained HFE-7500 fluorinated oil (3M, Germany) with 1.4 wt % perfluoropolyether−polyethylene glycol (PFPE−PEG) fluorosurfactants (Ran Biotechnologies, Inc.) and 10.5 mM PFPE−carboxylic acid (Krytox, MW, 7000−7500/mol, DuPont, Germany). Note that the Krytox-concentration can be estimated *via* a Rhodamine 6G assay (see the Supporting Information, Figure S5). This combination of lipid composition, buffer conditions, and Krytox concentration will be referred to as the "standard conditions". These were employed unless otherwise specified. A volume of 100 μL of aqueous solution was layered on top of 300 μL of the oil−surfactant mix. Note that the reaction volumes are scalable as long as the oil−surfactant mix is used in excess (to form oil-in-water droplets, the volumetric ratio of oil to aqueous phase has to be reversed). The probe was vortexed vigorously for about 10 s until water-in-oil droplets formed (visible as a milky emulsion layer on top of the remaining oil). Note that emulsion droplets will form independent of the shaking method, manual shaking, vortexing, or with an emulsification processor. The latter, however, will produce

DOI: 10.1021/acssynbio.9b00034
ACS Synth. Biol. 2019, 8, 937−947

mainly GUVs with a diameter below 10 μm (see the Supporting Information, Figure S9). The SUVs fuse to form a spherical supported lipid bilayer at the droplet periphery.[21] To release the GUVs from the oil phase, 100 μL of the aqueous solution (10 mM $MgCl_2$, 30 mM Tris, pH 7.4, or an osmolarity-matched buffer) is pipetted on top of the droplet layer. To destabilize the droplets, 100 μL of perfluoro-1-octanol (PFO) destabilizing agent (Sigma-Aldrich, Germany) was added slowly. Within seconds to minutes, the milky emulsion breaks up and disappears, forming a transparent aqueous layer on top of the oil−surfactant mix. From this top layer, the released GUVs were carefully removed with a pipet and transferred into a BSA-coated observation chamber (bovine serum albumin, SERVA Electrophoresis GmbH, Germany) for immediate imaging or stored in a fresh test tube at 4 °C for up to 48 h. For imaging purposes, it can be beneficial to sediment the GUVs in a glucose/sucrose gradient to prevent them from moving during the observation. For FRAP measurements and dye influx experiments, we therefore supplemented the buffer containing the SUVs with 200 mM sucrose and released the GUVs into an osmolarity-matched buffer containing glucose. By omitting $MgCl_2$ in the release buffer, it is possible to prevent adhesion of the GUVs to one another and to prevent fusion with the coverslide. Note that while immediate release is possible, the release efficiency can be improved by overnight storage of the dsGUVs at 4 °C for equilibration purposes before addition of the release buffer and the destabilizing agent.

Confocal Fluorescence Microscopy. For the confocal imaging, two different confocal laser scanning microscope setups were used: a Leica TCS SP5 confocal (Leica Microsystems GmbH, Germany) with a 40× water immersion objective (HC PL APO 40×/1.10 w, CORR CS2, Leica Microsystems GmbH, Germany) and a Zeiss LSM 800 confocal (Carl Zeiss AG, Germany) with a 20× air objective (Plan-Apochromat 20×/0.8 M27, Carl Zeiss AG, Germany) and a 63× oil immersion objective (Plan-Apochromat 63×/1.40 Oil DIC, Carl Zeiss AG, Germany). In both setups, the pinhole aperture was set to one Airy Unit, and experiments were performed at room temperature. The recorded images were brightness and contrast adjusted and analyzed with ImageJ (NIH).

FRAP Measurements. For FRAP measurements, the same Leica SP5 confocal microscope was used as described above, equipped with an argon laser (Leica Microsystems GmbH, Germany). The GUVs were sealed in an observation chamber, where they quickly settled on the bottom of the coverslide aided by a glucose/sucrose gradient. A bleaching spot with a radius of 2.5 μm was defined at the confocal plane at the top of the GUV. Using the FRAP-WIZZARD, 8 images were recorded before bleaching (laser intensity, 20%), 10 images during bleaching (laser intensity, 80%), and 30 images after bleaching (laser intensity, 20%) as indicated in Figure 3A. The 256 pixel × 256 pixel images were acquired at a line rate of 1 kHz. The diffusion coefficient was derived from the recorded images using a custom-written MATLAB (MathWorks, Inc.) code as described previously.[21]

CryoTEM. Samples were prepared for cryo-EM by applying 2.5 μL of GUVs solution (20% EggPG, 79% EggPC, 1% LissRhod-PE in PBS, 10 mM $MgCl_2$) onto a glow-discharged 200 mesh C-flat holey carbon-coated multihole grid (Protochips, Morrisville, NC). The grid was blotted for 4 s and plunge-frozen in liquid ethane using a Vitrobot Mark IV (FEI NanoPort, Eindhoven, The Netherlands) at 100% humidity and stored under liquid nitrogen. Cryo-EM specimen grids were imaged on a FEI Tecnai G2 T20 twin transmission electron microscope (FEI NanoPort, Eindhoven, The Netherlands) operated at 200 kV. Electron micrographs were recorded with a FEI Eagle 4k HS, 200 kV CCD camera with a total dose of ≈40 electrons/Å^2. Images were acquired at 50 000× nominal magnification with 1.24 μm defocus applied.

Dye Influx Experiments. Droplet stabilized GUVs were produced from an aqueous solution containing SUVs (2 mM 69% EggPC, 30% EggPG, 1% LissRhod-PE), 10 mM $MgCl_2$, 200 mM sucrose, 10 mM Tris, and 1 mM EDTA and an oil phase containing HFE-7500 fluorinated oil, 1.4 wt % PEG-based fluorosurfactant, and 10.5 mM Krytox. The GUVs were released into an aqueous buffer containing 230 mM glucose, 10 mM Tris, and 1 mM EDTA. Just before the measurement, the aqueous solution containing the GUVs was mixed in a ratio of 9:1 with an aqueous solution containing 70 μM fluorescein, 230 mM glucose, 10 mM Tris, 1 mM EDTA, and 10.7 nM heptameric α-hemolysin nanopores (75 nM monomers). For the control experiment, the α-hemolysin was omitted. The final solution was pipetted into an observation chamber, sealed, and imaged as described with the Zeiss 800 confocal laser scanning microscope.

Zeta Potential Measurements. The zeta potentials of GUVs and SUVs were measured with a Malvern ZetaSizer Nano ZS in phosphate buffered saline in a folded capillary zeta cell (Malvern). The refractive index for the dispersant was set to 1.330, and the viscosity to 0.882 cP with a dielectric constant of 79. The $\kappa \cdot a$ value was set to 1.5. The particle refractive index was set to 1.42 (matching the refractive index of the GUVs). For each condition, 3 measurements were performed with a minimum of 10 runs per measurement. The maximal voltage was set to 25 V in order to reduce the oxidation/reduction effect of the lipid at the capillary electrodes. Raw data was processed and fitted with the build in general propose mode. For washing, the water phase of the released GUVs was diluted into phosphate buffered saline and pelleted at 18 000g for 30 min. The supernatant was discarded, and the pellet was resuspended in an equivalent amount of magnesium-free PBS. For confocal fluorescence images before and after centrifugation, see the Supporting Information Figure S9. It should be noted, however, that larger GUVs do not remain intact when centrifuged at that speed. The GUV solutions were diluted 1:10 to a final volume of 1 mL at 25 °C with 5 min equilibration time.

Reconstitution and Encapsulation. *Integrin Reconstitution.* Integrin $\alpha_{IIb}\beta_3$ was purified by Christine Mollenhauer from outdated human blood platelets (Katharinenhospital Stuttgart) based on a protocol described earlier[46] and optimized by Stojan Perisic. The purified integrin was used for fluorescence labeling by means of a NHS (succiniminidyl) ester-conjugated Alexa Fluor 568 fluorescent dye (Life Technologies, Germany). The protein was stored at −80 °C. The reconstitution of the purified integrin into SUVs was carried out according to a previously published protocol.[47] In brief, 435 μM eggPC and 435 μM eggPG were dried under a gentle stream of nitrogen and then placed in a desiccator under vacuum for 2 h or overnight. Next, the dried lipids and Alexa Fluor 568-labeled $\alpha_{IIb}\beta_3$ integrin were dissolved in 1 mL of 20 mM Tris-HCl pH 7.4, 50 mM NaCl, 1 mM $CaCl_2$, and 0.1% Triton X-100 to a final ratio of 1:1000 (integrin/lipid). Then the solution was incubated on a Thermomixer (Eppendorf,

DOI: 10.1021/acssynbio.9b00034
ACS Synth. Biol. 2019, 8, 937−947

Germany) for 2 h at 37 °C and 600 rpm shaking (Eppendorf ThermoMixer C, Germany). Afterward, 50 mg/mL BT Bio-Beads SM-2 (BIO-RAD, Germany) for detergent removal were added into the microtube. The mixture was stirred on a magnetic stirrer for 3.5 h. This step was repeated once more in order to remove the Triton X-100 completely. The proteoliposome solution was used immediately for dsGUV formation or stored up to 3.5 h at 4 °C. In order to create integrin proteo-GUV, the integrin proteoliposomes were mixed 1:10 with SUVs (27.25% DOPC, 27.25% POPC, 30% DOPG, 15% cholesterol, and 0.5% Atto488 DOPE) to a final lipid concentration of 1.1 mM in 20 mM Tris-HCl, pH 7.4, 50 mM NaCl, 1 mM $CaCl_2$, and 10 mM $MgCl_2$. This liposome mixture was used as an aqueous phase for dsGUV formation.

Cholesterol-Tagged DNA. HPLC purified 3′ cholesterol-tagged DNA with a 5′ Cy3 label was purchased from Integrated DNA Technologies, Inc. (Belgium, DNA sequence: 5′ GAT GCA TAG AAG GAA 3′). It was added to preformed SUVs at a concentration of 1 μM, where it self-assembles into the lipid membrane. The DNA-functionalized SUVs were used to form GUVs *via* the shaking method under the standard conditions.

Pyranine Encapsulation. 8-Hydroxypyrene-1,3,6-trisulfonic acid trisodium salt (pyranine) was purchased from Merck (Germany) and encapsulated at a concentration of 100 nM under the standard conditions.

mRNA Encapsulation. VEGFD mRNA was generously provided by Prof. Daniela Mauceri (Interdisciplinary Center for Neurosciences, Heidelberg). The RNA solution was diluted to a final concentration of 1 ng/μL in a 3 mM SUV solution (30% DOPC, 69% POPC, 1% LissRhod-PE). The obtained lipid mix was used as the aqueous phase to form GUVs *via* the shaking method under the standard conditions. For image acquisition, released RNA containing GUVs were incubated with 0.5× SYBR Green I (Sigma-Aldrich S9430, Germany) for 30 min and imaged as previously described.

Polystyrene Beads Encapsulation. Polybead Polystyrene Microspheres with a diameter of 1 μm were purchased from Polysciences, Inc. (North America) and added at a concentration of 10^8 beads/to the aqueous phase for GUV formation. The excitation wavelength used for imaging under the confocal microscope was 405 nm.

Mitochondria Encapsulation. Total mitochondrial extracts were obtained from MitoTracker Green FM (Thermo Fischer Scientific, Germany)-labeled HeLa cells using the mitochondrial isolation kit from Thermo Fischer Scientific (89874) strictly following the manufacturer's instructions. The mitochondria containing solution was mixed 1:10 with a 3 mM lipid solution (SUVs composed of 30% DOPC, 69% POPC, 1% LissRhod-PE) in PBS and 10 mM $MgCl_2$. The obtained lipid mix was used as the aqueous phase to form GUVs *via* the shaking method under the standard conditions.

E. coli. GFP-labeled *E. coli* were suspended in PBS at OD = 10 and mixed at a ratio of 1:1 with 3 mM SUVs (30% DOPG, 34.75% DOPC, 34.75% POPC, 0.5% Atto488-DOPE). The mixture was used as an aqueous phase for the formation of GUVs *via* the shaking method described before.

GUVs Encapsulation. GUVs with internal GUVs were formed using a similar strategy as for the multicompartment systems encapsulating SUVs (Figure 1B,v). Positively charged SUVs were encapsulated together with negatively charged GUVs in the absence of Mg^{2+} ions. Under these conditions, the positively charged liposomes fuse at the droplet periphery, whereas negatively charged liposomes remain inside the droplet lumen.

Lipid Tubulation. Lipid tubulation was achieved by osmotic deflation of the GUVs after release as described previously for GUVs made by electroformation.[42] Briefly, a small drop of GUV solution was exposed to air, causing evaporation and hence a slow increase in salt concentration on the GUV's exterior. The resulting osmotic pressure leads to water eflux from the GUVs and hence their deflation.

■ ASSOCIATED CONTENT

Supporting Information

The Supporting Information is available free of charge on the ACS Publications website at DOI: 10.1021/acssynbio.9b00034.

Step-by-step instructions for the shaking method for GUV formation; choosing an appropriate lipid concentration; control experiment with uncharged surfactants; dynamic light scattering experiments; quantification of the amount of GUVs produced *via* the shaking method; rhodamine 6G partitioning experiment; variation of lipid composition and buer conditions; α-hemolysin dye influx experiment; comparison of zeta potentials of SUVs and GUVs; and GUVs before and after centrifugation (PDF)

Video S1, protocol of the shaking method for GUV formation (AVI)

Video S2, dye influx experiments (AVI)

Video S3, osmotic deflation of GUVs made by the shaking method (AVI)

■ AUTHOR INFORMATION

Corresponding Authors

*E-mail: ilia.platzman@mr.mpg.de.

*E-mail: spatz@mr.mpg.de.

ORCID

Kerstin Göpfrich: 0000-0003-2115-3551

Ilia Platzman: 0000-0003-1239-7458

Notes

The authors declare no competing financial interest.

■ ACKNOWLEDGMENTS

The authors acknowledge funding from the European Research Council, Grant Agreement No. 294852, SynAd and the MaxSynBio Consortium, which is jointly funded by the Federal Ministry of Education and Research of Germany and the Max Planck Society. The authors acknowledge the financial support by the Federal Ministry of Education and Research of Germany (BMBF) within the Project PolyAntiBak (Grant 13XP5073A). They also acknowledge the support from the SFB 1129 of the German Science Foundation and the VolkswagenStiftung (priority call "Life?"). J.P.S. is the Weston Visiting Professor at the Weizmann Institute of Science and part of the Excellence Cluster CellNetworks at the University of Heidelberg. K.G. received funding from the European Union's Horizon 2020 Research and Innovation Program under the Marie Skłodowska-Curie Grant Agreement No. 792270. O.S. acknowledges the support from the Heidelberg Bioscience International Graduate School. The authors thank Christine Mollenhauer for providing purified integrin, Stojan Persic for optimizing the integrin purification protocol, and

DOI: 10.1021/acssynbio.9b00034
ACS Synth. Biol. 2019, 8, 937−947

Daniela Mauceri for providing the mRNA. The Max Planck Society is appreciated for its general support.

REFERENCES

(1) Akbarzadeh, A., Rezaei-Sadabady, R., Davaran, S., Joo, S. W., and Zarghami, N. (2013) Liposome: classification, preparation, and applications. *Nanoscale Res. Lett. 8*, 1.
(2) Göpfrich, K., Platzman, I., and Spatz, J. P. (2018) Mastering Complexity: Towards Bottom-up Construction of Multifunctional Eukaryotic Synthetic Cells. *Trends Biotechnol. 36*, 938−951.
(3) Szostak, J. W., Bartel, D. P., and Luisi, P. L. (2001) Synthesizing life. *Nature 409*, 387−390.
(4) Schwille, P., and Diez, S. (2009) Synthetic biology of minimal systems synthetic biology of minimal systems. *Crit. Rev. Biochem. Mol. Biol. 44*, 223−242.
(5) Powell, K. (2018) Biology from Scratch. *Nature 563*, 172−175.
(6) Reeves, J. P., and Dowben, R. M. (1969) Formation and properties of thin-walled phospholipid vesicles. *J. Cell. Physiol. 73*, 49−60.
(7) Weinberger, A., Tsai, F. C., Koenderink, G. H., Schmidt, T. F., Itri, R., Meier, W., Schmatko, T., Schröder, A., and Marques, C. (2013) Gel-assisted formation of giant unilamellar vesicles. *Biophys. J. 105*, 154−164.
(8) Angelova, M. I., and Dimitrov, D. S. (1986) Liposome electroformation. *Faraday Discuss. Chem. Soc. 81*, 303.
(9) Steinkühler, J., De Tillieux, P., Knorr, R. L., Lipowsky, R., and Dimova, R. (2018) Charged giant unilamellar vesicles prepared by electroformation exhibit nanotubes and transbilayer lipid asymmetry. *Sci. Rep. 8*, 11838.
(10) Ingolfsson, H. I., Melo, M. N., van Eerden, F. J., Arnarez, C., Lopez, C. A., Wasse- naar, T. A., Periole, X., de Vries, A. H., Tieleman, D. P., and Marrink, S. J. (2014) Lipid Organization of the Plasma Membrane. *J. Am. Chem. Soc. 136*, 14554−14559.
(11) Moscho, A., Orwar, O., Chiu, D. T., Modi, B. P., and Zare, R. N. (1996) Rapid preparation of giant unilamellar vesicles. *Proc. Natl. Acad. Sci. U. S. A. 93*, 11443−11447.
(12) Pautot, S., Frisken, B. J., and Weitz, D. A. (2003) Production of Unilamellar Vesicles Using an Inverted Emulsion. *Langmuir 19*, 2870−2879.
(13) Morales-Penningston, N. F., Wu, J., Farkas, E. R., Goh, S. L., Konyakhina, T. M., Zheng, J. Y., Webb, W. W., and Feigenson, G. W. (2010) GUV preparation and imaging: Minimizing artifacts. *Biochim. Biophys. Acta, Biomembr. 1798*, 1324−1332.
(14) Walde, P., Cosentino, K., Engel, H., and Stano, P. (2010) Giant Vesicles: Preparations and Applications. *ChemBioChem 11*, 848−865.
(15) Noireaux, V., and Libchaber, A. (2004) A vesicle bioreactor as a step toward an artificial cell assembly. *Proc. Natl. Acad. Sci. U. S. A. 101*, 17669−17674.
(16) Nishimura, K., Tsuru, S., Suzuki, H., and Yomo, T. (2015) Stochasticity in Gene Expression in a Cell-Sized Compartment. *ACS Synth. Biol. 4*, 566−576.
(17) Richmond, D. L., Schmid, E. M., Martens, S., Stachowiak, J. C., Liska, N., and Fletcher, D. A. (2011) Forming giant vesicles with controlled membrane composition, asym- metry, and contents. *Proc. Natl. Acad. Sci. U. S. A. 108*, 9431−6.
(18) Deshpande, S., Caspi, Y., Meijering, A. E. C., and Dekker, C. (2016) Octanol-assisted liposome assembly on chip. *Nat. Commun. 7*, 10447.
(19) Matosevic, S., and Paegel, B. M. (2013) Layer-by-layer cell membrane assembly. *Nat. Chem. 5*, 958−963.
(20) Deng, N.-N., Yelleswarapu, M., Zheng, L., and Huck, W. T. S. (2017) Microfluidic Assembly of Monodisperse Vesosomes as Artificial Cell Models. *J. Am. Chem. Soc. 139*, 587−590.
(21) Weiss, M., Frohnmayer, J. P., Benk, L. T., Haller, B., Heitkamp, T., Börsch, M., Dimova, R., Sundmacher, K., Vidakovic-Koch, T., Lipowsky, R., Bodenschatz, E., Baret, J. C., Platzman, I., and Spatz, J. P. (2018) Sequential bottom-up assembly of mechanically stabilized synthetic cells by microfluidics. *Nat. Mater. 17*, 89−96.
(22) Haller, B., Göpfrich, K., Schröter, M., Janiesch, J.-W., Platzman, I., and Spatz, J. P. (2018) Charge-controlled microfluidic formation of lipid-based single-and multicompartment systems. *Lab Chip 18*, 2665−2674.
(23) Gach, P. C., Iwai, K., Kim, P., Hillson, N. J., and Singh, A. K. (2017) Droplet Microfluidics for Synthetic Biology. *Lab Chip 17*, 3388−3400.
(24) Cremer, P. S., Groves, J. T., Kung, L. A., and Boxer, S. G. (1999) Writing and Erasing Barriers to Lateral Mobility into Fluid Phospholipid Bilayers. *Langmuir 15*, 3893−3896.
(25) Richter, R. P., and Brisson, A. R. (2005) Following the Formation of Supported Lipid Bilayers on Mica: A Study Combining AFM, QCM-D, and Ellipsometry. *Biophys. J. 88*, 3422−3433.
(26) Richter, R. P., Berat, R., and Brisson, A. R. (2006) Formation of Solid-Supported Lipid Bilayers: An Integrated View. *Langmuir 22*, 3497−3505.
(27) Biner, O., Schick, T., Müller, Y., and von Ballmoos, C. (2016) Delivery of membrane proteins into small and giant unilamellar vesicles by charge-mediated fusion. *FEBS Lett. 590*, 2051−2062.
(28) Carrara, P., Stano, P., and Luisi, P. L. (2012) Giant Vesicles “”Colonies: A Model for Primitive Cell Communities. *ChemBioChem 13*, 1497−1502.
(29) Saito, A. C., Ogura, T., Fujiwara, K., Murata, S., and Nomura, S.-i. M. (2014) Introducing Micrometer-Sized Artificial Objects into Live Cells: A Method for CellGiant Unil- amellar Vesicle Electrofusion. *PLoS One 9*, No. e106853.
(30) Ramadurai, S., Holt, A., Krasnikov, V., van den Bogaart, G., Killian, J. A., and Poolman, B. (2009) Lateral Diffusion of Membrane Proteins. *J. Am. Chem. Soc. 131*, 12650−12656.
(31) Song, L., Hobaugh, M. R., Shustak, C., Cheley, S., Bayley, H., and Gouaux, J. E. (1996) Structure of staphylococcal alpha-hemolysin, a heptameric transmembrane pore. *Science 274*, 1859−1866.
(32) Berube, B. J., and Wardenburg, J. B. (2013) Staphylococcus aureus -Toxin: Nearly a Century of Intrigue. *Toxins 5*, 1140−1166.
(33) Chiba, M., Miyazaki, M., and Ishiwata, S. (2014) Quantitative Analysis of the Lamellarity of Giant Liposomes Prepared by the Inverted Emulsion Method. *Biophys. J. 107*, 346−354.
(34) Jørgensen, I. L., Kemmer, G. C., and Pomorski, T. G. (2017) Membrane protein reconstitution into giant unilamellar vesicles: a review on current techniques. *Eur. Biophys. J. 46*, 103−119.
(35) Majumder, S., Willey, P. T., DeNies, M. S., Liu, A. P., and Luxton, G. W. G. (2019) A synthetic biology platform for the reconstitution and mechanistic dissection of LINC complex assembly. *J. Cell Sci. 132*, jcs219451.
(36) Ritzmann, N., Thoma, J., Hirschi, S., Kalbermatter, D., Fotiadis, D., and Müller, D. J. (2017) Fusion Domains Guide the Oriented Insertion of Light-Driven Proton Pumps into Li- posomes. *Biophys. J. 113*, 1181−1186.
(37) Göpfrich, K., Zettl, T., Meijering, A. E. C., Hernández-Ainsa, S., Kocabey, S., Liedl, T., and Keyser, U. F. (2015) DNA-tile structures lead to ionic currents through lipid membranes. *Nano Lett. 15*, 3134−3138.
(38) Göpfrich, K., Li, C.-Y., Ricci, M., Bhamidimarri, S. P., Yoo, J., Gyenes, B., Ohmann, A., Winterhalter, M., Aksimentiev, A., and Keyser, U. F. (2016) Large-Conductance Transmembrane Porin Made from DNA Origami. *ACS Nano 10*, 8207−14.
(39) Langecker, M., Arnaut, V., Martin, T. G., List, J., Renner, S., Mayer, M., Dietz, H., and Simmel, F. C. (2012) Synthetic Lipid Membrane Channels Formed by Designed DNA Nanos- tructures. *Science 338*, 932−936.
(40) Franquelim, H. G., Khmelinskaia, A., Sobczak, J.-P., Dietz, H., and Schwille, P. (2018) Membrane sculpting by curved DNA origami scaffolds. *Nat. Commun. 9*, 811.
(41) Jahnke, K., Weiss, M., Frey, C., Antona, S., Janiesch, J.-W., Platzman, I., Göpfrich, K., and Spatz, J. P. (2019) Programmable Functionalization of Surfactant-Stabilized Microfluidic Droplets via DNA-Tags. *Adv. Funct. Mater.*, 1808647.

DOI: 10.1021/acssynbio.9b00034
ACS Synth. Biol. 2019, 8, 937−947

(42) Okano, T., Inoue, K., Koseki, K., and Suzuki, H. (2018) Deformation Modes of Giant Unilamellar Vesicles Encapsulating Biopolymers. *ACS Synth. Biol. 7*, 739−747.
(43) Gobbo, P., Patil, A. J., Li, M., Harniman, R., Briscoe, W. H., and Mann, S. (2018) Programmed assembly of synthetic protocells into thermoresponsive prototissues. *Nat. Mater. 17*, 1145.
(44) Clark, I. C., Thakur, R., and Abate, A. R. (2018) Concentric electrodes improve microfluidic droplet sorting. *Lab Chip 18*, 710.
(45) Ding, R., Ung, W. L., Heyman, J. A., and Weitz, D. A. (2017) Sensitive and predictable separation of microfluidic droplets by size using in-line passive filter. *Biomicrofluidics 11*, No. 014114.
(46) Fitzgerald, L. A., Leung, B., and Phillips, D. R. (1985) A method for purifying the platelet mem- brane glycoprotein IIb-IIIa complex. *Anal. Biochem. 151*, 169−177.
(47) Erb, E. M., Tangemann, K., Bohrmann, B., Muller, B., and Engel, J. (1997) Integrin cdi,63 re- constituted into lipid bilayers is nonclustered in its activated state but clusters after fibrinogen binding. *Biochemistry 36*, 7395−7402.

DOI: 10.1021/acssynbio.9b00034
ACS Synth. Biol. 2019, 8, 937−947